International Journal of Engineering

Journal Homepage: www.ije.ir

Numerical Study and Comparison of Two-dimensional Ferrofluid Flow in Semi-porous Channel under Magnetic Field

P. Jalili[a], M. D. Afifi[b], B. Jalili[*a], A. M. Mirzaei[b], D. D. Ganji[b]

[a] Department of Mechanical Engineering, North Tehran Branch, Islamic Azad University, Tehran, Iran
[b] Department of Mechanical Engineering, Babol Noshirvani University of Technology, Babol, Iran

A B S T R A C T

In this article, the equations governing the constant ferromagnetic current are investigated. The Lorentz force restrains this ferrofluid flow in a semi-porous valve. Analyzes were performed on three sub-particle fluids: kerosene and blood, water and magnetite. Modeling in the Cartesian coordinate system using the relevant equations was investigated. A slight thinning should be considered in the lower part of this channel. This research has used two Akbari-Ganji methods (AGM) and finite element method (FEM) to solve the equations. Nonlinear differential equations are solved using the above two methods. In the finite element model, the effect of changing the Hartmann number and the Reynolds number on the flow velocity and the derivatives of the velocity and shear stress of the fluid were investigated. As the Hartmann number increases, the velocity decreases in both directions. The Reynolds number changes in different slip parameters, which shows the opposite behavior for the two directions. Also, the insignificant effect of volume fraction of nanoparticles on velocity and its derivatives and shear stress was investigated. The results of solving the equations with the above two methods were compared with HAM. The results obtained using AGM and FEM and their comparison with previous researches have led to complete agreement, which shows the efficiency of the techniques used in this research.

NOMENCLATURE

L_x	characteristic length [m]		P	dimensionless pressure [$= hq/\nu_f$]
u,v	dimensionless velocity components		p^*	hydrostatic pressure [kgm^{-1} s^{-2}]
x,y	dimensionless variables		**Greek Symbols**	
U,V	dimensionless velocity		β	slip parameter [$= l/h$]
u^*,v^*	velocity vector components in x* and y* directions, respectively [ms^{-1}]		υ	kinematic viscosity [m^2 s^{-1}]
x^*,y^*	spatial coordinates [m]		ρ	density [kgm^{-3}]
h	channel's width [m]		σ	electrical conductivity [s m^{-1}]
u_0	x velocity of plate [ms^{-1}]		ε	the ratio of h and L$_x$
l	slip length [m]		ϕ	nanoparticle volume fraction
B	constant magnetic field [m^{-1} A]		μ	dynamic viscosity [kgm^{-1} s^{-1}]
Re	Reynolds number		**Subscripts**	
Ha	Hartmann number [$= Bh\sqrt{\sigma/\mu_f}$]		s	nano-solid particles
q	transpiration velocity		f	base fluid
			nf	nanofluid

1. INTRODUCTION

Recently, the wide and abundant use of non-Newtonian fluids in industry and engineering sciences has caused

them to pay special attention to these materials. The characteristic and importance of this type of fluid can be seen in polymer compounds and edible substances. Ferrofluid is one of the non-Newtonian fluids that has

*Corresponding Author Email: b.jalili@iau-tnb.ac.ir (B. Jalili)

recently been investigated by scientists. The physical structure of this fluid is very complex and no model can fully show all its features. For these reasons, investigation and analysis of the behavior of ferrofluid is very important.

Abbas et al. [1] investigated second-order fluid in the presence of a chemical reaction in a semi-porous channel. In this research, homotopy method was used to approximate analytical solution of the differential equations. Abdel Rahim and Rahman [2] analyzed heat transfer and fluid mass transfer in a magnetic field, which was assumed to be slow flow under electric conduction. Abbas and Hasnain [3], Abbas et al. [4, 5] have conducted studies on a two-phase fluid flow in an entirely porous medium. In this research, magnetite (Fe_3O_4) fluid was selected, and the sliding flow of nanomaterials in an inclined channel with thermal radiation was investigated and analyzed.

For the investigation of fluid properties, it can be mentioned that the fluid in the semi-porous channel is chemically conductive, and the mass transfer of the fluid is second-order with chemical reaction, Abbas et al. [6] investigated Maxwell fluid flow with radiation in an axisymmetric semi-porous channel. The natural convection micropolar fluid flow problem developed by Ashmawy [7]. According to that study, it was observed that the enhancement of the micropolar parameter includes the decrease or an increase in the fluid velocity. There are various medical mechanisms, such as blood circulation in the veins, the presence of oxygen generators in the blood, blood dialysis in the artificial kidney, and various types of engineering activities such as filter design; all of these mechanisms, despite the presence of a fluid flow in a channel semi-porous flows, it can be analyzed and investigated. Ayaz [8] used it for nonlinear ordinary differential equations. Also, in electrical engineering, new problems are presented, which are linear and nonlinear. It should also be noted that solving the governing equations of medical flow using DTM was investigated by Bég et al. [9]. One of the most effective analyses of fluid flow inside the channel is presented by Berman [10]. This article gives equations governing the smooth flow of a rectangular channel with semi-porous walls.

To fully describe a fluid flow in Manal with porous walls, solving the Navier-Stokes equations in two-dimensional laminar flow was necessary. This work was done by Brinkman [11], which is clearly shown the dependence of pressure and velocity components on fluid properties and channel dimensions. Due to the development and evolution of components, researchers are trying to create a variety of advanced fluids. These types of fluids should be closer to the real state in terms of heat exchange. For this purpose, they focused their studies on nanofluids because nanofluids release nano-sized particles. Chen and Ho [12] extended DTM to solve

partial differential equations. Therefore, using these materials in liquids can achieve lower thermal conductivity. Choi and Eastman [13], Choi et al. [14] proposed the first idea for these advanced fluids and discussed the extraordinary physical and chemical properties of these fluids that ferrofluids are also considered part of these fluids.

Ghasemian et al. [15] investigated forced displacement heat transfer on magnetite and numerically compared them with the presence of fluid under constant and alternating fields. Analysis of the flow of two fluids with the same density and varying viscosity in a horizontal channel and an unsteady state was recorded by Ghosh et al. [16]. According to this study, when the viscous fluid is near the channel, it is unstable for many parameters. Koriko et al. [17] conducted studies on the importance of partial slip and buoyancy on the boundary flow of a nanofluid, where the viscosity was considered to be zero. The equations governing nanoparticles were solved using the classic Runge-Kutta method; they found that it can be concluded that the maximum flow velocity occurs in larger values of partial slip and buoyancy parameters. We need analytical approximations often broken nonlinearly to solve nonlinear problems. Liao [18] mentioned the homotopy method in his book and solved difficult nonlinear problems with the help of this method. Mousavi et al. [19] investigated the hydrodynamic behavior of ferrofluid with 3D simulation in a wave channel and used the mathematical model with matching magnetohydrodynamics and ferro hydrodynamics to formulate the problem. Also, this research investigated the efficacy of changes in the Nusselt number and the amount of magnetic gradient. The use of semi-numerical techniques such as the homotopy analysis method (HAM) and differential transform method (DTM) has been presented by Parsa et al. [20]. They solved the governing equations of fluid flow in a semi-porous channel and investigated the effect of some parameters, such as Reynolds and Hartmann numbers in the heat transfer rate.

With the help of this method in an analytical function and using unknown and known boundary conditions, the derivative of n can be calculated at a known point. Rashidi et al. [21, 22] by using the differential transform method (DTM), were able to provide a solution for studying a non-Newtonian fluid flow inside a channel with semi-porous boundaries. This research was done using the parametric perturbation method. Salehpour and Ashjaee [23] investigated on the ferrofluid flow in a miniature channel under alternating and constant fields in a two-dimensional space. They found that the constant magnetic field enhancement heat transfer and the heat transfer rate decreases with increasing Reynolds number. They also calculated the optimal frequency for maximum heat transfer at high Reynolds numbers. In addition to that, Sanyal and Sanyal [24] studied on the two-

dimensional steady flow in an inclined rectangular channel with the presence of a magnetic field. From the outcomes of this research, we can refer to the graphical comparison of velocity, temperature, and magnetic field numerically. Also, the fluid flow has been investigated as a two-dimensional steady Maxwell flow in a symmetric semi-porous channel with a heat transfer rate. By using DTM and a semi-numerical solution with Taylor series expansion, Zhou [25] has formulated such existing problems.

The composition of ferrofluid includes substances such as Ferrum (Fe_3O_4) and suspension liquid of nanoparticles in several domains. Due to surface tension between solid particles and traditional fluid, a coating such as surfactants can be used to reduce it. If there is a magnetic field next to these particles, their behavior differs from ordinary metals. Also, these particles become magnetized inside the magnetic field. The location of the fluid under the magnetic force can be affected. Insomuch, the response of the ferrofluid to the external magnetic field is evident. One of the characteristics of sub-fluids is that they have very small particles. This makes them maintain their position and not settle down despite the magnetic force for a long time. In fact, papers and researches on ferrofluid flow in non-repetitive geometries are very limited.

Abbas et al. [26] developed a steady ferrofluid flow study in a semi-porous channel. In this research, fluids such as water, kerosene, blood, and magnetite are subjected to the Lorentz force in a semi-porous channel. The solution methods in this paper are the homotopy analysis method (HAM), differential transformation method (DTM), and Runge-Kutta method. The efficacy of Hartmann and Reynolds number changes on the flow velocity is shown and analyzed. Jalili et al. [27] investigated ferrofluid microstructure and inertial characteristics using homotopy and Akbari-Ganji methods. Also, the efficacy of related parameters on flow performance, temperature, and velocity has been analyzed. It should be noted that the fluid velocity in the vicinity of the sheet and at a distance from the sheet has been compared. In a study with a semi-analytical solution method on the Lorentz force and the efficacy of viscosity on nanofluid, the viscosity is variable, and the temperature parameter changes in a linear function. The semi-analytical AGM is used in this paper presented by Jalili et al. [28]. Changes in fluid velocity have been investigated by changing parameters such as Prantel, Hartmann, and Nusselt numbers. In another study conducted by Jalili et al. [29], the performance of magnetohydrodynamic heat transfer in a porous circular chamber was analyzed using Darcy's law. Also, by using the eddy current function formula and solving it numerically, a good comparison has been made with FEM. This material is placed in a magnetic field under a horizontal magnetic force, and its behavior has been investigated with changes in the volume fraction of nanoparticles, inclination angle, Lorentz, and buoyancy forces. The use of three methods of comparing them to investigate the characteristics of a ferrofluid on a shrinking plate was demonstrated in a research conducted by Jalili et al. [30], which are AGM, FEM, and HPM. The base fluid in it is water and Fe_3O_4. According to this paper, it can be seen that the boundary and magnetic parameters have the same efficacy on the fluid velocity. This is not the case for the micro-rotation parameter.

Recent studies have investigated the nanofluid flow between two parallel plates under magnetic and electric fields in a rotating system. According to the research conducted by Jalili et al. [31], the velocity profile and micro-rotation velocity increased with the magnetic and rotation parameters also increased. Also, the efficacy of changes in Reynolds, Prantel, and Schmidt numbers, thermophoretic parameters, and Brownian motion have been analyzed.

Jalili et al. [32] conducted a study on a two-dimensional viscous fluid located between two porous spaces in a calm and incompressible manner. Based on this research, the equations between two discs have been solved using the Akbari-Ganji and finite element methods. With the help of the findings, the velocity, pressure, and temperature parameters have been analyzed. Also, sliding in the boundaries and changing the Reynolds number causes changes in the fluid velocity, which are obvious.

In the article presented by Jalili et al. [33], all heat transfer processes in non-Newtonian fluid flow have been investigated. AGM and FEM methods have been used to solve this fluid flow's governing equations, showing complete agreement. Several values for Hartmann number and electromagnetic force affect the velocity profiles. Also, an extensie analytical research has been done in this field [34-36].

As a result, the general approach of this article and research is to provide numerical and semi-numerical solutions for ferrofluid flow in a semi-porous channel under a magnetic field with two basic fluids such as water and kerosene. Finally, the fluid velocity is obtained in its final form by solving the relevant equations with three homotopy methods: the Akbari-Ganji and finite element methods. Also, comparing these three different techniques and the efficacy of fixed parameters on fluid velocity are analyzed.

The use of other numerical and experimental solution methods such as Euler, Taylor, and RK-4 methods can also be used to solve the governing equations of fluid flow. The very good agreement of the obtained results from the used methods is one of the advantages of adopting this approach in this article. The error caused by the mentioned methods is very small and negligible and finally it is acceptable.

A comprehensive literature above motivated us to investigate and analyze a ferrofluid flow in a transverse magnetic field (see Figure 1). In the continuation of this research, the effect of changes in Reynolds and Hartmann numbers, velocity slip parameter and volume fraction of nanoparticles is shown using the finite element method. The results help the readers to have a better understanding of the effect of the above parameters on the velocity profile, velocity derivatives and ferrofluid shear stress in two directions. The comparison of the values obtained from the present research with other researches is presented in order to show the validity of the proposed solution methods.

2. FORMULATION OF PROBLEM AND BASIC EQUATION

According to Figure 1, two infinitely rigid parallel plates located at a distance h from each other, where the desired fluid enters this range (see Figure 1). The slip condition is applied on the plate of length L_x along the x*-axis at $y^* = 0$. The rate of transpiration in an infinite porous plate is equal to q. The physical properties of the flow are two-dimensional, steady, and slow flow.

Water and kerosene-carrying magnetite Fe_3O_4 are two fluids considered nanoparticles in this research. Applying a magnetic field with intensity B is assumed in the desired channel. The magnetic field is transverse to the fluid flow. The effects of the induced magnetic field are not taken into account. Considering the above assumptions, the equations governing the flow are as follows [19, 20].

$$\frac{\partial u^*}{\partial x^*} + \frac{\partial v^*}{\partial y^*} = 0 \tag{1}$$

$$u^*\frac{\partial u^*}{\partial x^*} + v^*\frac{\partial u^*}{\partial y^*} =$$
$$-\frac{1}{\rho_{nf}}\frac{\partial p^*}{\partial x^*} + \frac{\mu_{nf}}{\rho_{nf}}(\frac{\partial^2 u^*}{\partial x^{*2}} + \frac{\partial^2 u^*}{\partial y^{*2}}) - \frac{u^*\sigma B^2}{\rho_{nf}} \tag{2}$$

$$u^*\frac{\partial v^*}{\partial x^*} + v^*\frac{\partial v^*}{\partial y^*} =$$
$$-\frac{1}{\rho_{nf}}\frac{\partial p^*}{\partial x^*} + \frac{\mu_{nf}}{\rho_{nf}}(\frac{\partial^2 v^*}{\partial x^{*2}} + \frac{\partial^2 v^*}{\partial y^{*2}}) \tag{3}$$

Also, the effective dynamic viscosity is calculated as follows [11]:

$$\mu_{nf} = \frac{\mu_f}{(1-\phi)^{2.5}}$$

The nanoparticle volume fraction is represented by the symbol ϕ (<0.05 for most practical cases). The shape of the particles can be considered spherical or non-
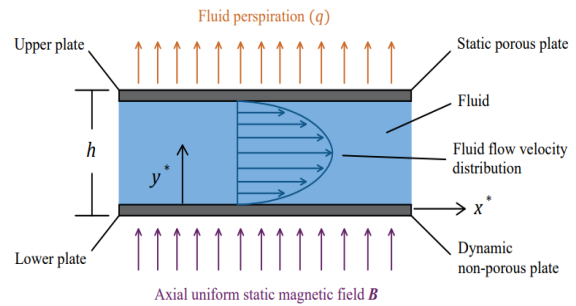

Figure 1. An overview of the physics of the problem

spherical. It should be noted that the effective density has been analysed by Mousavi et al. [19].

The physical properties of magnetic nanoparticles and the base fluid are shown in Table 1 [17-19].

$$\rho_{nf} = \rho_f(1-\phi) + \rho_s$$

In specific situations, the boundary conditions (BCs) are as follows:

$$y^* = 0 : u^* = u_0^* + \frac{\partial u^*}{\partial y}, v^* = 0, y^* = h : u^* = 0, v^* = -q, \tag{4}$$

Scientists and researchers are trying to investigate the conditions of the sliding velocity of Navier in the walls and their use. Some articles and research that have used these boundary conditions as well [1, 3, 7, 16, 24].

Using the following equation, the average velocity $U(y)$ is calculated)

$$Uh = \int_0^h u^* dy^* = L_x q \tag{5}$$

With the help of the following non-dimensional variables, solutions to the problem can be found.

$$x = \frac{x^*}{L_x}, y = \frac{y^*}{h}, u = \frac{u^*}{U}, v = \frac{v^*}{q}, P_y = \frac{p^*}{\rho q^2}. \tag{6}$$

By substituting the above variables in Equations (1), (3), and (6) is obtained

$$\frac{\partial u}{\partial x} + \frac{\partial v}{\partial y} = 0 \tag{7}$$

$$u\frac{\partial u}{\partial x} + v\frac{\partial u}{\partial y} = -\varepsilon^2\frac{\partial P_y}{\partial x} - u\frac{Ha^2}{Re((1-\phi+\phi(\frac{\rho_s}{\rho_f})))}$$
$$+\frac{1}{Re}(\frac{1}{(1-\phi)^{2.5}(1-\phi+\phi(\frac{\rho_s}{\rho_f}))})(\varepsilon^2\frac{\partial^2 u}{\partial x^2} + \frac{\partial^2 u}{\partial y^2}) \tag{8}$$

$$u\frac{\partial v}{\partial x} + v\frac{\partial v}{\partial y} = -\frac{\partial P_y}{\partial y}$$
$$+\frac{1}{Re}(\frac{1}{(1-\phi)^{2.5}(1-\phi+\phi(\frac{\rho_s}{\rho_f}))})(\varepsilon^2\frac{\partial^2 v}{\partial x^2} + \frac{\partial^2 v}{\partial y^2}) \tag{9}$$

TABLE 1. Physical properties of magnetic nanoparticles

Physical property	Water	Kerosene	Blood	Fe_3O_4
Density(ρ)	997	783	1050	5180
Viscosity(μ)	0.001003	0.00164	0.003-0.004	-

Hartmann and Reynolds numbers in Equations (8) and (9) are equal to:

$$Ha = Bh\sqrt{\frac{\sigma}{\mu_f}} \quad Re = \frac{hq}{\upsilon_f}$$

The term ε, is very tiny because it is the ratio of h and L_x. To remove ε from Equations (8) and (9), Berman [10] similarity transformations are used

$$u = u^* U^{-1} = x\frac{dV}{dx} + u_0 U(y), v = -V(y). \tag{10}$$

According to the above relationships, it can be seen that in Equation (9), the quantity $\partial P_y/\partial y$ is independent of the x variable. According to Equation (8), it can be said that $\partial^2 P_y/\partial x^2$ is not a function of the longitudinal variable x. If the asterisks are ignored for ease of work, the following relationships will appear after changing the variables

$$V'^2 + VV'' - \frac{1}{Re}\left(\frac{1}{(1-\phi)^{2.5}(1-\phi+\phi(\frac{\rho_s}{\rho_f}))}\right)V'''$$
$$+ \frac{Ha^2}{Re(1-\phi+\phi(\frac{\rho_s}{\rho_f}))}V' = \varepsilon^2\frac{\partial^2 P_y}{\partial x^2} = \varepsilon^2\frac{1}{x}\frac{\partial P_y}{\partial x}. \tag{11}$$

$$\begin{cases} u(x) = u_0, u'(x) = u_1, \dots, u^{(m-1)}(x) = u_{m-1} & at\ x = 0 \\ u(x) = u_{L_0}, u'(x) = u_{L_1}, \dots, u^{(m-1)}(x) = u_{L_{m-1}} & at\ x = L \end{cases} \tag{17}$$

In Equation (17), a series of order n is assumed according to the boundary conditions at $x = L$, where the coefficients are considered constant. This series is written as the answer to the first differential equation as follows:

$$u(x) = \sum_{i=0}^{n} a_i x^i = a_0 + a_1 x^1 + a_2 x^2 + \cdots + a_n x^n \tag{18}$$

In order to enhance the accuracy in solving Equation (16), it is necessary to enhance the series expressions in Equation (18). Due to the order of the above series being n, there are $(n + 1)$ unknown coefficients, which we usually need $(n + 1)$ equations to solve. In Equation

$$\begin{cases} u(L) = a_0 + a_1 L + a_2 L^2 + \cdots + a_n L^n = u_{L_0} \\ u'(L) = a_1 + 2a_2 L + 2a_3 L^2 + \cdots + na_n L^{n-1} = u_{L_1} \\ u''(L) = 2a_2 + 6a_3 L + 12a_4 L^2 + \cdots + n(n-1)a_n L^{n-2} = u_{L_{m-1}} \\ \vdots \quad \vdots \quad \vdots \quad \vdots \quad \vdots \quad \vdots \quad \vdots \quad \vdots \end{cases} \tag{20}$$

$$UV' - VU' = \frac{1}{Re}\left(\frac{1}{(1-\phi+\phi(\frac{\rho_s}{\rho_f}))}\right)\left(\frac{U''}{(1-\phi)^{2.5}} - Ha^2 U\right). \tag{12}$$

If Equation 11 is calculated in terms of variable y, it will be as follows:

$$V^{iv} = (1-\phi)^{2.5}(Ha^2 V''$$
$$+ Re((1-\phi+\phi(\frac{\rho_s}{\rho_f})))(V'V'' - VV''')). \tag{13}$$

The boundary conditions governing the equations are written as follows:

$$V(0) = 0, V'(0) = \beta V''(0), U(0) = 1 + \beta U'(0). \tag{14}$$

$$V(1) = 1, V'(1) = 0, U(1) = 0. \tag{15}$$

where $\beta = l/h$.

3. THE GENERALITIES OF AKBARI GANJI'S METHOD (AGM)

Considering the boundary conditions, the differential equations are as follows:

$$p_k: f(u, u', u'', \dots, u^{(m)}) = 0; u = u(x) \tag{16}$$

The p function in a nonlinear differential equation is assumed as a function of u. Also, the u parameter is considered a function of x and its derivatives. In this way, the boundary conditions of the equations are established as follows:

(17), boundary conditions are applied for the $(n + 1)$ equation.

3. 1. Apply BCs with AGM
Boundary conditions are used to solve Equation (18) as follows
When $x = 0$:

$$\begin{cases} u(0) = a_0 = u_0 \\ u'(0) = a_0 = u_0 \\ u''(0) = a_2 = u_2 \\ \vdots \quad \vdots \quad \vdots \end{cases} \tag{19}$$

and when $x = L$:

After inserting Equation (20) into Equation (16) and applying boundary conditions in differential Equation (16), it is obtained based on the following technique:

$$p_0: f\left(u(0), u'(0), u''(0), \dots, u^{(m)}(0)\right)$$
$$p_1: f\left(u(L), u'(L), u''(L), \dots, u^{(m)}(L)\right) \tag{21}$$

According to the selection of n $(n < m)$ terms from Equation (18), to create a set of equations consisting of $(n + 1)$ equations and $(n + 1)$ unknowns, there will be additional unknowns. Therefore, to solve this problem, due to these additional unknowns in the mentioned equations, m times should be derived from Equation (23), and then the BCs should be applied to them. The solution process in Flowchart 1 has been fully investigated.

$$p'_k: f\left(u', u'', u''', \dots, u^{(m+1)}\right)$$
$$p''_k: f\left(u'', u''', u^{(IV)}, \dots, u^{(m+2)}\right) \tag{22}$$

$$\vdots \quad \vdots \quad \vdots \quad \vdots \quad \vdots$$

In Equation (22), the boundary conditions are applied to the derivatives of the differential equation p_k.

$$p'_k: \begin{cases} f\left(u'(0), u''(0), u'''(0), \dots, u^{(m+1)}(0)\right) \\ f\left(u'(L), u''(L), u'''(L), \dots, u^{(m+1)}(L)\right) \end{cases} \tag{23}$$

$$p''_k: \begin{cases} f\left(u''(0), u'''(0), u^{(IV)}(0), \dots, u^{(m+2)}(0)\right) \\ f\left(u''(L), u'''(L), u^{(IV)}(L), \dots, u^{(m+2)}(L)\right) \end{cases} \tag{24}$$

$(n + 1)$ equation is obtained from Equations (19) to (24), so $(n + 1)$ unknown coefficient in Equation (18),

including $a_0, a_1, \dots, a_n$ will be calculated. Solving the nonlinear differential Equation (16) is done by calculating the coefficients of Equation (18).

3. 2. Solving Equations Governing Fluid Flow with AGM   In this method, using appropriate functions, polynomial series with constant coefficients can be considered:

$$U = \sum_{i=0}^{5} a_i x^i$$
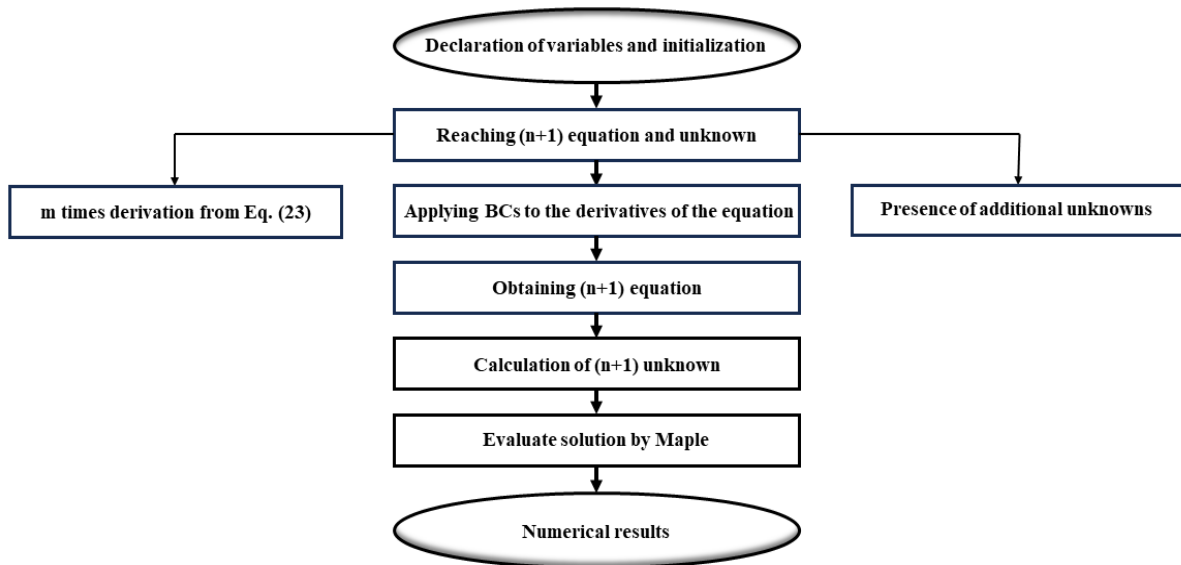$$U = x^5 a_5 + x^4 a_4 + x^3 a_3 + x^2 a_2 + x a_1 + a_0 \tag{25}$$

$$V = \sum_{i=0}^{5} b_i x^i$$
$$V = x^5 b_5 + x^4 b_4 + x^3 b_3 + x^2 b_2 + x b_1 + b_0 \tag{26}$$

Equations (12) and (13) are written as follows:

$$U * diff\,(V, x) - V * diff\,(U, x) =$$
$$\frac{1}{Re}\left(\frac{1}{\left(1 - \phi + \phi\left(\frac{\rho_s}{\rho_f}\right)\right)}\right)\left(\frac{diff\,(U, x, x)}{(1 - \phi)^{2.5}} - Ha^2 * U\right)$$

$$diff\,(V, x, x, x, x) = (1 - \phi)^{2.5}(Ha^2 * diff\,(V, x, x)$$
$$+ Re\left((1 - \phi + \phi\left(\frac{\rho_s}{\rho_f}\right))\right)(diff\,(V, x)$$
$$* diff\,(V, x, x) - V * diff\,(V, x, x, x))).$$

The use of BCs in Equations (14) and (15) is as follows:

Flowchart 1. Showing the process of solving equations with AGM

$$V(0) = 0 \rightarrow b_0 = 0 \tag{27}$$

$$V'(0) = \beta * V''(0) \rightarrow b_1 = 0.4b_2 \tag{28}$$

$$U(0) = 1 + \beta * U'(0) \rightarrow a_0 = 1 + 0.2a_1 \tag{29}$$

$$V(1) = 1 \rightarrow b_5 + b_4 + b_3 + b_2 + b_1 + b_0 = 1 \tag{30}$$

$$V'(1) = 0 \rightarrow 5b_5 + 4b_4 + 3b_3 + 2b_2 + b_1 = 0 \tag{31}$$

$$U(1) = 0 \rightarrow a_5 + a_4 + a_3 + a_2 + a_1 + a_0 = 0 \tag{32}$$

According to the considered series in Equations (25) and (26), there are 12 unknown coefficients. Therefore, 12 equations are needed. Six equations are obtained by applying boundary conditions, and six more equations are added as follows:

$$\begin{aligned} S\,7 &= F(0) \rightarrow S\,7 = a_0 b_1 - a_1 b_0 \\ &= 1.895700084 a_2 - 0.8558895353 a_0 \end{aligned} \tag{33}$$

$$\begin{aligned} S\,8 &= F'(0) \rightarrow S\,8 = 2a_0 b_2 - 2a_2 b_0 \\ &= 5.687100252 a_3 - 0.8558895353 a_1 \end{aligned} \tag{34}$$

$$\begin{aligned} S\,9 &= F''(0) \rightarrow S\,9 = 6a_0 b_3 + 2a_1 b_2 - 2a_2 b_1 - 6a_3 b_0 \\ &= 22.74840102 a_4 - 1.711779071 a_2 \end{aligned} \tag{35}$$

$$\begin{aligned} S\,10 &= F'''(0) \rightarrow S\,10 = 24a_0 b_4 + 12a_1 b_3 - 12a_3 b_1 - 24a_4 b_0 \\ &= 113.7420050 a_5 - 5.135337212 a_3 \end{aligned} \tag{36}$$

$$\begin{aligned} S\,11 &= G(0) \rightarrow S\,11 = 24b_4 \\ &= 1.805959798 b_2 + 2.110038414 b_1 b_2 - 6.330115242 b_0 b_3 \end{aligned} \tag{37}$$

$$\begin{aligned} S\,12 &= G'(0) \rightarrow S\,12 = 120b_5 \\ &= 50417879393 b_3 + 4.220076828 b_2^2 - 25.32046097 b_0 b \end{aligned} \tag{38}$$

Finally, the values of V and U are equal to:

$V = 0.03526533002 x^5 + 0.2595824095 x^4$
$-1.884935683 x^3 + 1.850062816 x^2 + 0.7400251266 x$
$U = 0.2981496437 x^5 - 0.5758048195 x^4 + 0.2737060224 x^3$
$+0.6157135630 x^2 - 1.343137008 x + 0.7313725984$

4. RESULTS AND DISCUSSION

Equations (12) and (13) were solved with AGM and FEM to obtain velocity fields $V(y), V'(y), U(y), U'(y), \tau_V$ and τ_U according to Equations (14) and (15). Drawing and displaying graphs $V(y), V'(y), U(y), U'(y), \tau_V$ and τ_U and the efficacy of changes in relevant parameters have

been done in them. Figure 2 shows $V(y), V'(y), U(y), U'(y), \tau_V$ and τ_U profiles. Also, the comparison of three solution methods AGM, FEM, and HAM has been done when $Re = Ha = 1.0, \beta = 0.2$ and $\phi = 0.04$. By comparing the figures, it can be concluded that the outcome obtained from all methods are very close to each other. This result proves and confirms the validity of the methods.
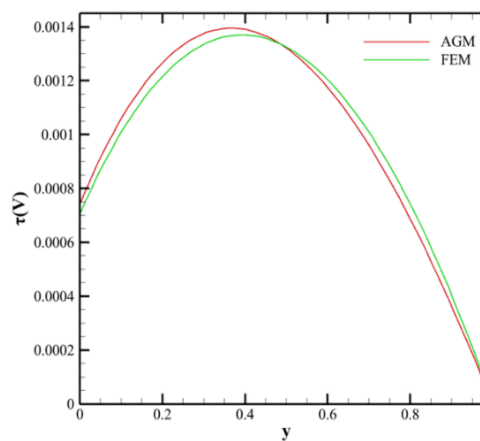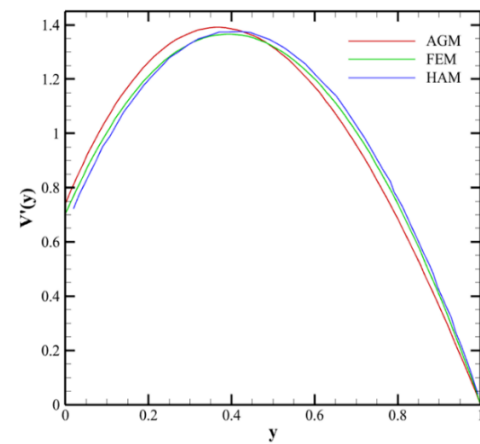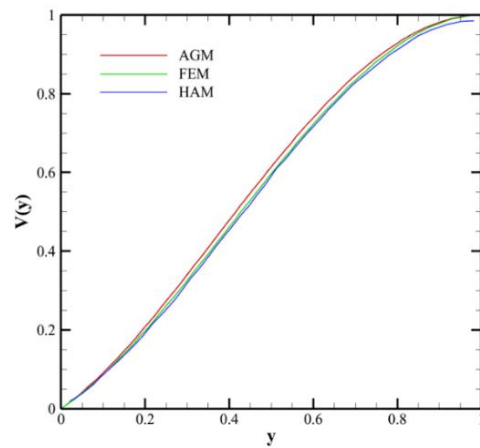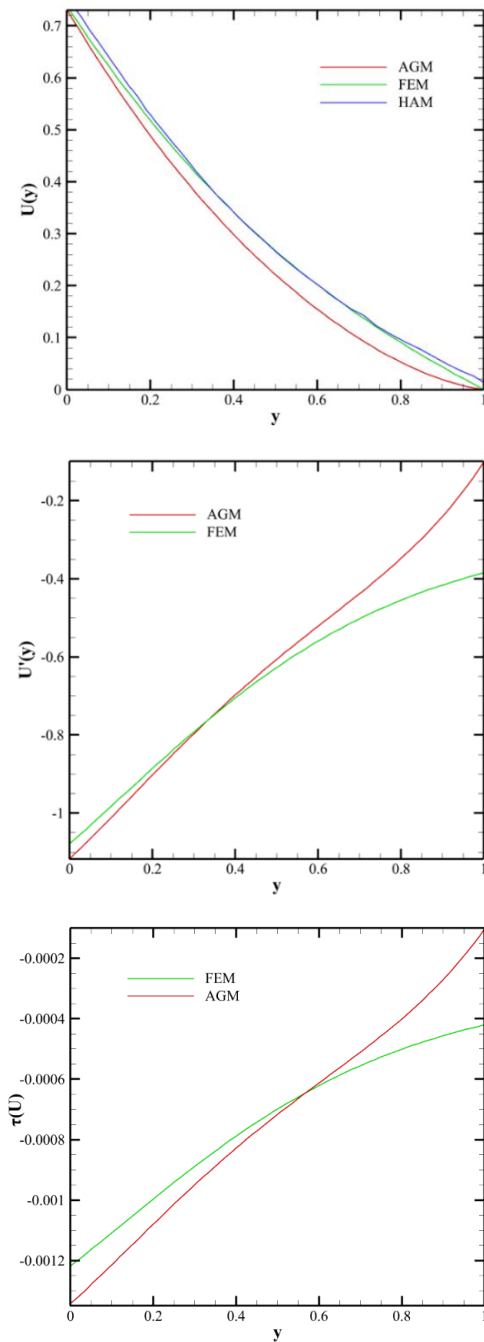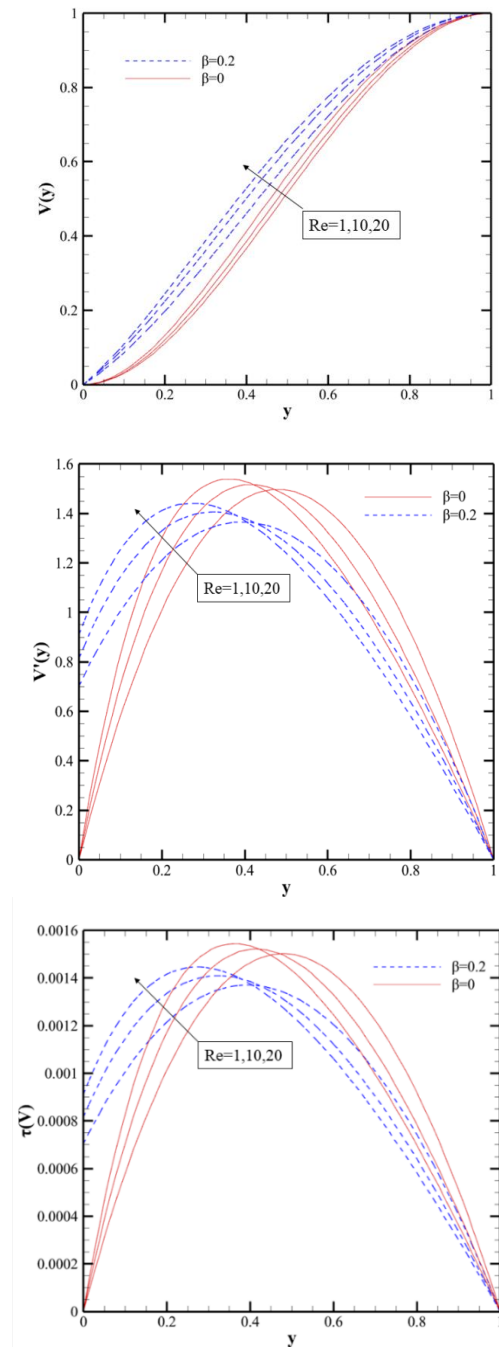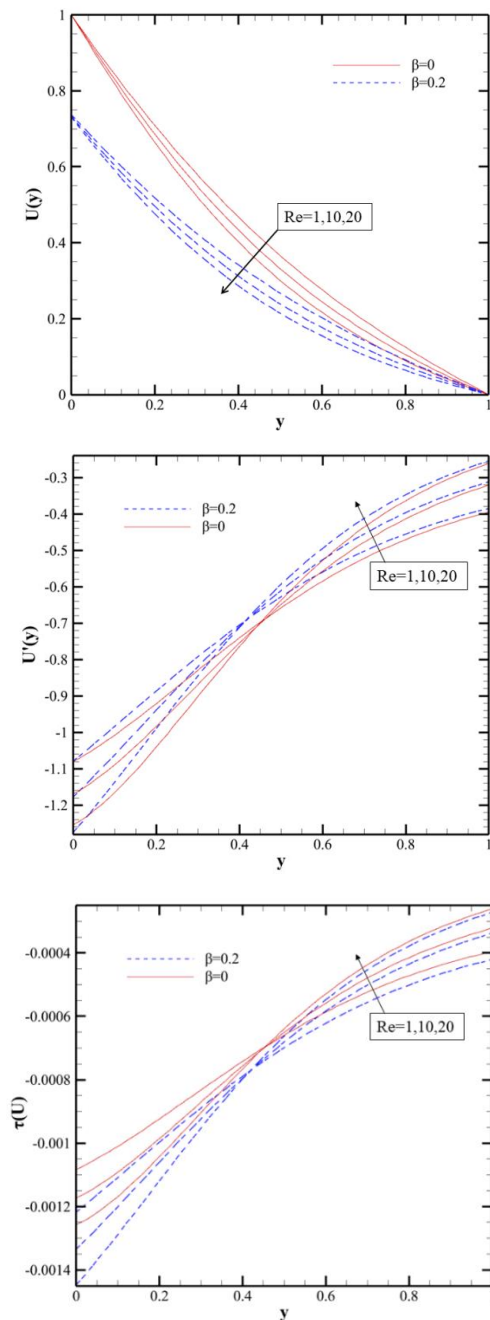
Figure 2. Comparison of the conclusion obtained for $V(y), V'(y)$ and $U(y)$ with three methods of AGM, FEM, HAM, and comparison of $U'(y), \tau_V$ and τ_U with two methods of AGM and FEM where $Re = Ha = 1.0, \phi = 0.04, \beta = 0.2$

plane increases and the fluid flow approaches the upper plane as an outcome. Decreasing the velocity in the x-direction $U(y)$ and increasing the velocity in the y-direction $V(y)$ is the outcome of the previous movement. By increasing the Reynolds number from 1 to 20, the velocity enhancement in the y-direction and the velocity decrease in the x-direction are tangible. Also, according to Figure 3, it can be seen that with the enhancement of the Reynolds number, $V'(y)$ also increases. But when approaching the top page ($y = 0.45$), it shows a reverse

Changes in $V(y), V'(y), U(y), U'(y), \tau_V$ and τ_U for fixed values of $\phi = 0.04$ and $Ha = 1.0$ and several values of Re with two boundary conditions of slip and no-slip are shown in Figure 3. With the enhancement of Reynolds number, the flux of the side body on the upper
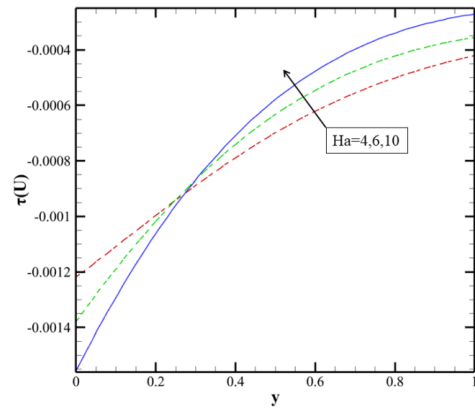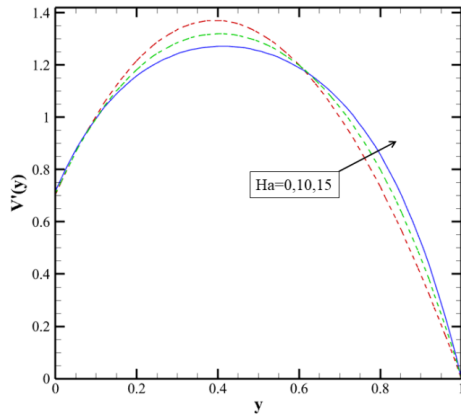
be seen that there is no difference in the efficacy of Reynolds number changes in the boundary conditions of sliding and non-slipping.

According to Figure 4, the distribution of fluid flow velocity decreases with the enhancement of the Hartmann number. This decrease is much higher in $U(y)$. The Lorentz force enters in the x-direction because the magnetic field is placed in the y-direction. Thus, the magnetohydrodynamic force generated in $V(y)$ and $V'(y)$ can be ignored, although it plays a significant role in $U(y)$ and $U'(y)$. With an increase in Hartmann's number in the range of $0 \leq y \leq 0.6$, a decrease in $V'(y)$ can be seen, and in $0.6 \leq y \leq 1$, the value of $V'(y)$ increases. This behavior is also shown in shear stress (τ_V). The algebraic value of $U'(y)$ in the range of $0 \leq y \leq 0.4$ increases with an increase in Hartmann's number, but its value is negative. In the range of $0.4 \leq y \leq 1$, its behavior is reversed and the same process is repeated for τ_U in a smaller order.

The efficacy of ϕ sub-particle volume fraction and β slip on fluid flow velocity distribution $V(y)$ and $U(y)$ Likewise Re and ϕ are shown in Figure 5. Also, in the vicinity of the upper and lower plates, for boundary conditions with slip and no-slip, the opposite behavior can be observed for $V'(y)$ and $U'(y)$. If the volume fraction of nanoparticles (ϕ) increases, $V(y)$ decreases and $U(y)$ increases. This behavior is similar for both velocity profiles with an increase in slip parameter (β). As the value of ϕ increases, in the range of $0 \leq y \leq 0.5$, the value of $V'(y)$ and the algebraic value of $U'(y)$ decrease, and then at $0.5 \leq y \leq 1$, the algebraic value of $U'(y)$ and $V'(y)$ increases. A similar behavior is also shown for shear stresses (τ_V and τ_U) in two directions.

Figures 6 and 7 show the effect of changes in Reynolds and Hartmann numbers and the volume fraction parameter of nanoparticles. As can be seen, with an increase in Reynolds number, $V(y)$ increases, but if the Hartmann number or volume fraction of nanoparticles increases, $V(y)$ decreases.
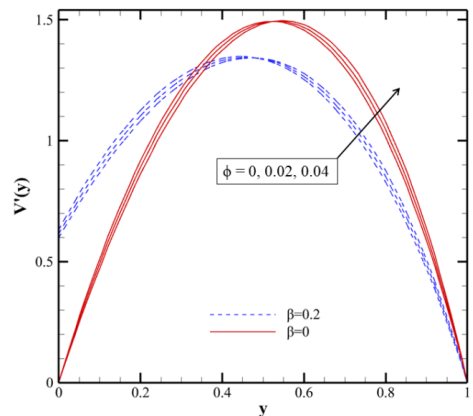

Figure 3. Comparison of diagrams obtained for $V(y), V'(y), U(y), U'(y), \tau_V$ and τ_U with FEM for several values of β and Re when $\phi = 0.04, Ha = 0.0$

behavior. But $U'(y)$ shows the opposite behavior. That is, in the range of $0 \leq y \leq 0.45$, with an increase in Reynolds number, $U'(y)$ decreases, and then it takes an increasing trend in $0.45 \leq y \leq 1$. Based on this, it can be concluded that the values of τ_U and τ_V also behave similar to the derivatives of velocity, because the constant coefficient (μ) is multiplied in the derivatives and shear stresses appear. According to Figure 3, it can
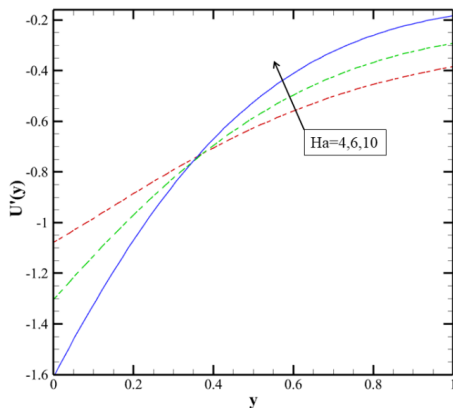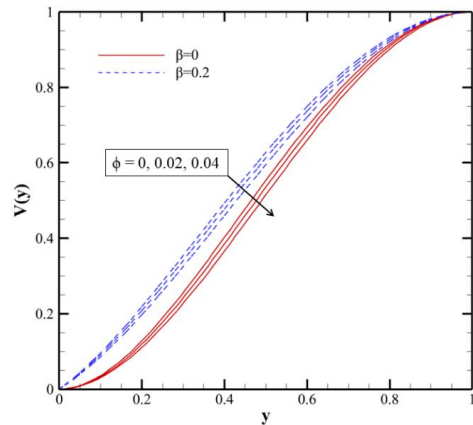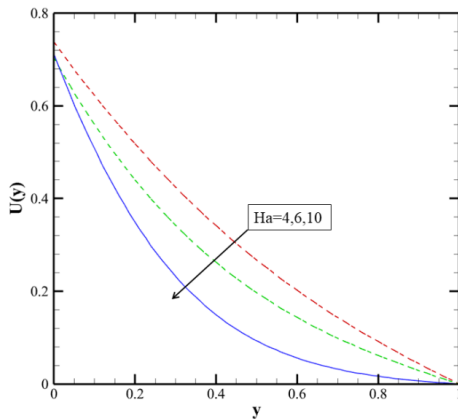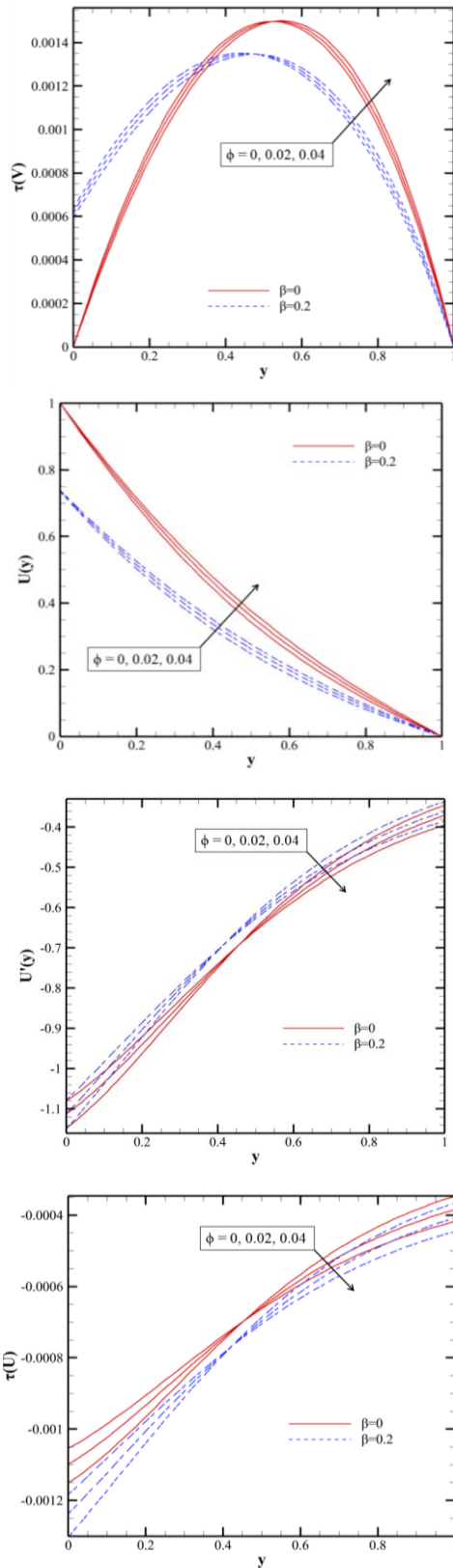
Figure 4. Comparison of $V(y), V'(y), U(y), U'(y), \tau_V$ and τ_U diagrams using FEM with several values for Ha when $Re = 1.0, \beta = 0.2, \phi = 0.04$
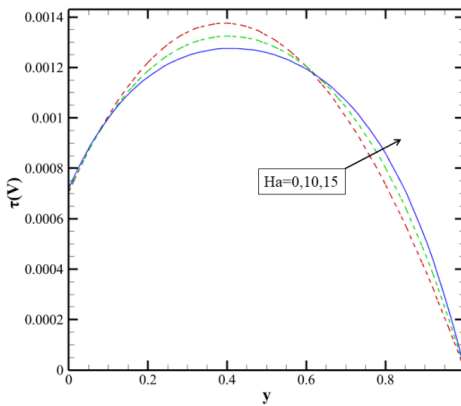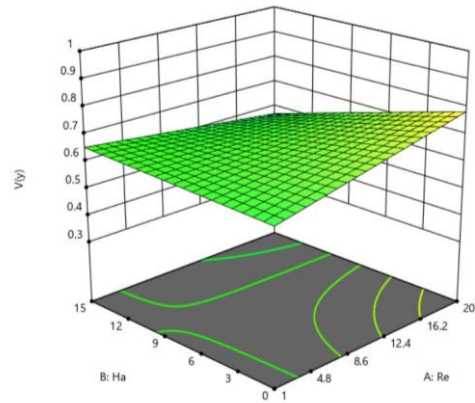
Based on Figures 8 and 9, it can be concluded that $U(y)$ decreases with an increase in Hartman and Reynolds numbers. But if the volume fraction of nanoparticles is increased, $U(y)$ increases.

Convergence for several values of $V(y), U(y), \tau_V$ and τ_U in terms of y is listed in Table 2 to 5. In Tables 2 and 3, the results obtained for the values of water velocity

Figure 6. Efficacy of changes in Reynolds number and Hartmann number on constant Phi number equal to 0.02

Figure 7. The efficacy of changes in Reynolds number and Phi number on the constant Hartmann number equal to 7.5

Figure 8. The efficacy of changes in Reynolds number and Hartmann number on constant Phi number is equal to 0.02
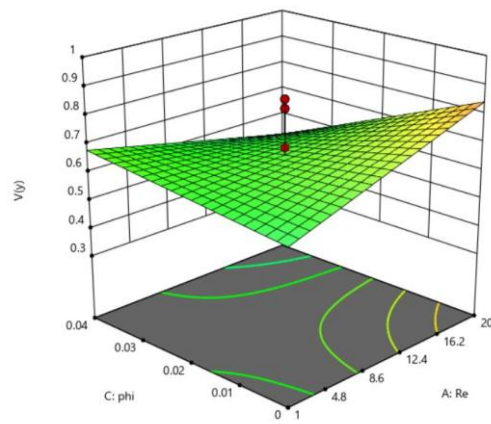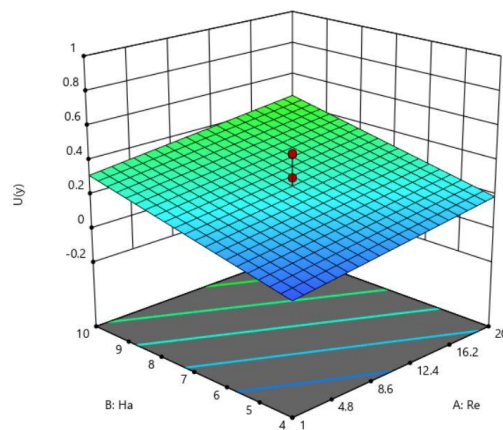
Figure 5. Comparison of $V(y), V'(y), U(y), U'(y), \tau_V$ and τ_U diagrams with FEM for several values of ϕ and β when $Re = Ha = 1.0$

in two directions in the current research with the two methods of AGM and FEM and the values obtained with

P. Jalili et al. / IJE TRANSACTIONS B: Applications Vol. 36 No. 11, (November 2023) 2087-2101
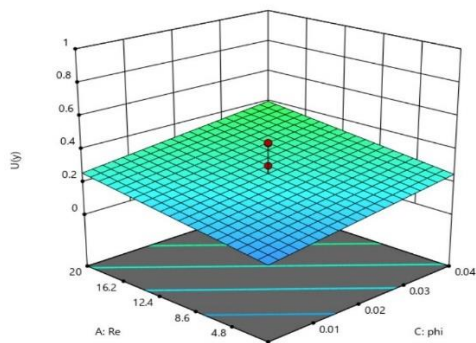
Figure 9. The efficacy of changes in Reynolds number and Phi number on Hartmann's constant number equal to 7

the three methods of HAM, DTM and Numerical are presented. The comparison of the present results and their correspondence with the results of other researches [26] shows the efficiency of the methods used in this article. In addition, in Tables 4 and 5, the values obtained from the current research with two AGM and FEM methods are given.

The changes related to the three parameters of Re, Ha and ϕ in a 3D space in the form of optimization are given in Figures 6 and 7 for $V(y)$.

The changes related to the three parameters of Re, Ha and ϕ in a 3D space in the form of optimization are given in Figures 8 and 9 for $U(y)$.

TABLE 2. The analogy of the obtained outcome for the velocity of $V(y)$ when $\phi = 0.04, Re = 1.0, Ha = 1.5, \beta = 0.3$ for the Water base.

y	AGM	FEM	HAM [26]	DTM [26]	Numerical solution [26]
0	0.000000	0.000000	0.000000	0.000000	0.000000
0.1	0.098899	0.097758	0.097758	0.097758	0.097758
0.2	0.220465	0.215312	0.215311	0.215312	0.215311
0.3	0.365673	0.344513	0.344742	0.344742	0.344742
0.4	0.498575	0.479145	0.478699	0.478699	0.478699
0.5	0.644486	0.610354	0.610245	0.610246	0.610245
0.6	0.754926	0.732942	0.732703	0.732703	0.732703
0.7	0.851991	0.839491	0.839514	0.839515	0.839514
0.8	0.932754	0.924120	0.924121	0.924122	0.924121
0.9	0.981562	0.979879	0.979879	0.979880	0.979879
1	1.000000	1.000000	1.000000	1.000000	1.000000

TABLE 3. The analogy of the obtained outcome for the velocity of $U(y)$ when $\phi = 0.04, Re = 1.0, Ha = 1.5, \beta = 0.3$ for the Water base.

y	AGM	FEM	HAM [26]	DTM [26]	Numerical solution [26]
0	0.619974	0.602783	0.620077	0.620077	0.620077
0.1	0.486728	0.498574	0.502367	0.502367	0.502367
0.2	0.379256	0.399492	0.401721	0.401721	0.401721
0.3	0.272567	0.315897	0.316599	0.316599	0.316599
0.4	0.182456	0.245170	0.245171	0.245171	0.245171
0.5	0.137496	0.185479	0.185479	0.185479	0.185479
0.6	0.102891	0.135577	0.135577	0.135577	0.135577
0.7	0.075286	0.093610	0.093624	0.093624	0.093624
0.8	0.045872	0.057189	0.057961	0.057961	0.057961
0.9	0.022378	0.026981	0.027150	0.027150	0.027150
1	0.000000	0.000000	0.000000	0.000000	0.000000

TABLE 4. The analogy of the obtained outcome for τ_V when $\phi = 0.04, Re = 1.0, Ha = 1.5, \beta = 0.3$ for the Water base

y	AGM	FEM
0	0.000749	0.000711
0.1	0.001080	0.001033
0.2	0.001279	0.001219
0.3	0.001374	0.001334
0.4	0.001390	0.001365
0.5	0.001320	0.001321
0.6	0.001160	0.001201
0.7	0.000943	0.000994
0.8	0.000704	0.000711
0.9	0.000385	0.000434
1	0.000000	0.000000

TABLE 5. The analogy of the obtained outcome for τ_U when $\phi = 0.04, Re = 1.0, Ha = 1.5, \beta = 0.3$ for the Water base

y	AGM	FEM
0	-0.001400	-0.001255
0.1	-0.001247	-0.001120
0.2	-0.001110	-0.001001
0.3	-0.000971	-0.000889
0.4	-0.000844	-0.000780
0.5	-0.000712	-0.000660
0.6	-0.000575	-0.000571
0.7	-0.000446	-0.000502
0.8	-0.000316	-0.000444
0.9	-0.000179	-0.000390
1	0.000000	-0.000349

5. CONCLUSION

One of the most important goals of this research was to investigate and analyze two-dimensional fluid flow in relation to sliding efficiency on a nanofluid with a porous wall. The equations governing the flow were solved with the mentioned simplifications and two methods. Among the achievements of this article, the following factors can be mentioned:

➢ The area of convergence in $V''(0)$ is larger than that of $U'(0)$.
➢ The difference in AGM, FEM, and HAM outcomes is negligible, and all three methods are acceptable.
➢ As the Reynolds number enhancement, the velocity of the $V(y)$ fluid increases. This is while it reduces with the enhancement of Hartmann's number.

➢ As the Hartmann and Reynolds numbers increase, $U(y)$ decreases.
➢ As the nanoparticle volume fraction parameter increases, $U(y)$ increases and $V(y)$ decreases.
➢ If there are changes for Hartmann, Reynolds numbers and volume fraction of nanoparticles, the opposite behavior is reported for the derivatives of velocity and shear stress in the range of $0 \leq y \leq 1$.

6. REFERENCES

1. Abbas, Z., Ahmad, B. and Ali, S., "Chemically reactive hydromagnetic flow of a second-grade fluid in a semi-porous channel", *Journal of Applied Mechanics and Technical Physics*, Vol. 56, (2015), 878-888. https://doi.org/10.1134/S0021894415050156

2. Abdel-Rahim, Y.M. and Rahman, M.M., "Laminar semi-porous channel electrically conducting flow under magnetic field, International Conference on Heat Transfer, Fluid Mechanics and Thermodynamics. (2014).

3. Abbas, Z. and Hasnain, J., "Two-phase magnetoconvection flow of magnetite (Fe3O4) nanoparticles in a horizontal composite porous annulus", *Results in Physics*, Vol. 7, (2017), 574-580. https://doi.org/10.1016/j.rinp.2016.12.022

4. Abbas, Z., Hasnain, J. and Sajid, M., "Mhd two-phase fluid flow and heat transfer with partial slip in an inclined channel", *Thermal Science*, Vol. 20, No. 5, (2016), 1435-1446. https://doi.org/10.2298/TSCI130327049A

5. Abbas, Z., Rahim, T. and Hasnain, J., "Slip flow of magnetite-water nanomaterial in an inclined channel with thermal radiation", *International Journal of Mechanical Sciences*, Vol. 122, (2017), 288-296. https://doi.org/10.1016/j.ijmecsci.2017.01.040

6. Abbas, Z., Naveed, M., Naeem, M. and Zia, Q., "Analytical investigation of a maxwell fluid flow with radiation in an axisymmetric semi-porous channel by parameterized perturbation method", *Journal of the Brazilian Society of Mechanical Sciences and Engineering*, Vol. 40, (2018), 1-8. https://doi.org/10.1007/s40430-018-0985-z

7. Ashmawy, E., "Fully developed natural convective micropolar fluid flow in a vertical channel with slip", *Journal of the Egyptian Mathematical Society*, Vol. 23, No. 3, (2015), 563-567. https://doi.org/10.1016/j.joems.2014.06.019

8. Ayaz, F., "Solutions of the system of differential equations by differential transform method", *Applied Mathematics and Computation*, Vol. 147, No. 2, (2004), 547-567. https://doi.org/10.1016/j.joems.2014.06.019

9. Bég, T., Rashidi, M., Bég, O.A. and Rahimzadeh, N., "Differential transform semi-numerical analysis of biofluid-particle suspension flow and heat transfer in non-darcian porous media", *Computer Methods in Biomechanics and Biomedical Engineering*, Vol. 16, No. 8, (2013), 896-907. doi: 10.1080/10255842.2011.643470.

10. Berman, A.S., "Laminar flow in channels with porous walls", *Journal of Applied Physics*, Vol. 24, No. 9, (1953), 1232-1235. https://doi.org/10.1063/1.1721476

11. Brinkman, H.C., "The viscosity of concentrated suspensions and solutions", *The Journal of Chemical Physics*, Vol. 20, No. 4, (1952), 571-571. https://doi.org/10.1063/1.1700493

12. Chen, C.o.K. and Ho, S.H., "Solving partial differential equations by two-dimensional differential transform method", *Applied Mathematics and Computation*, Vol. 106, No. 2-3, (1999), 171-179. https://doi.org/10.1016/S0096-3003(98)10115-7

13. Choi, S.U. and Eastman, J.A., *Enhancing thermal conductivity of fluids with nanoparticles*. 1995, Argonne National Lab.(ANL), Argonne, IL (United States).

14. Choi, S., Zhang, Z.G., Yu, W., Lockwood, F. and Grulke, E., "Anomalous thermal conductivity enhancement in nanotube suspensions", *Applied Physics Letters*, Vol. 79, No. 14, (2001), 2252-2254. https://doi.org/10.1063/1.1408272

15. Ghasemian, M., Ashrafi, Z.N., Goharkhah, M. and Ashjaee, M., "Heat transfer characteristics of fe3o4 ferrofluid flowing in a mini channel under constant and alternating magnetic fields", *Journal of Magnetism and Magnetic Materials*, Vol. 381, No., (2015), 158-167. https://doi.org/10.1016/j.jmmm.2014.12.078

16. Ghosh, S., Usha, R. and Sahu, K.C., "Absolute and convective instabilities in double-diffusive two-fluid flow in a slippery channel", *Chemical Engineering Science*, Vol. 134, No., (2015), 1-11. https://doi.org/10.1016/j.ces.2015.04.049

17. Koriko, O.K., Animasaun, I., Mahanthesh, B., Saleem, S., Sarojamma, G. and Sivaraj, R., "Heat transfer in the flow of blood-gold carreau nanofluid induced by partial slip and buoyancy", *Heat Transfer—Asian Research*, Vol. 47, No. 6, (2018), 806-823. https://doi.org/10.1002/htj.21342

18. Liao, S., "Beyond perturbation: Introduction to the homotopy analysis method, CRC press, (2003).

19. Mousavi, S.M., Biglarian, M., Darzi, A.A.R., Farhadi, M., Afrouzi, H.H. and Toghraie, D., "Heat transfer enhancement of ferrofluid flow within a wavy channel by applying a non-uniform magnetic field", *Journal of Thermal Analysis and Calorimetry*, Vol. 139, (2020), 3331-3343. https://doi.org/10.1007/s10973-019-08650-6

20. Parsa, A.B., Rashidi, M.M., Bég, O.A. and Sadri, S., "Semi-computational simulation of magneto-hemodynamic flow in a semi-porous channel using optimal homotopy and differential transform methods", *Computers in Biology and Medicine*, Vol. 43, No. 9, (2013), 1142-1153. https://doi.org/10.1016/j.compbiomed.2013.05.019

21. Rashidi, M., Keimanesh, M., Bég, O.A. and Hung, T., "Magnetohydrodynamic biorheological transport phenomena in a porous medium: A simulation of magnetic blood flow control and filtration", *International Journal for Numerical Methods in Biomedical Engineering*, Vol. 27, No. 6, (2011), 805-821. https://doi.org/10.1002/cnm.1420

22. Rashidi, M., Pour, S.M. and Laraqi, N., "A semi-analytical solution of micro polar flow in a porous channel with mass injection by using differential transform method", *Nonlinear Analysis: Modelling and Control*, Vol. 15, No. 3, (2010), 341-350. https://doi.org/10.15388/NA.15.3.14329

23. Salehpour, A. and Ashjaee, M., "Effect of different frequency functions on ferrofluid fhd flow", *Journal of Magnetism and Magnetic Materials*, Vol. 480, (2019), 112-131. https://doi.org/10.1016/j.jmmm.2019.02.045

24. Sanyal, D. and Sanyal, M., "Hydromagnetic slip flow with heat transfer in an inclined channel", *Czechoslovak Journal of Physics B*, Vol. 39, No. 5, (1989), 529-536. https://doi.org/10.1007/BF01597717

25. Zhou, J., *Differential transformation and its applications for electrical circuits*. 1986, Huazhong University Press, Wuhan, China.

26. Abbas, Z., Hasnain, J., Aly, S. and Sheikh, M., "Comparative analysis for partial slip flow of ferrofluid fe3o4 nanoparticles in a semi-porous channel", *Journal of King Saud University-Science*, Vol. 32, No. 5, (2020), 2646-2655. https://doi.org/10.1016/j.jksus.2020.05.007

27. Jalili, B., Sadighi, S., Jalili, P. and Ganji, D.D., "Characteristics of ferrofluid flow over a stretching sheet with suction and injection", *Case Studies in Thermal Engineering*, Vol. 14, (2019), 100470. https://doi.org/10.1016/j.csite.2019.100470

28. Jalili, B., Ganji, A.D., Jalili, P., Nourazar, S.S. and Ganji, D., "Thermal analysis of williamson fluid flow with lorentz force on the stretching plate", *Case Studies in Thermal Engineering*, Vol. 39, (2022), 102374. https://doi.org/10.1016/j.csite.2022.102374

29. Jalili, B., Sadighi, S., Jalili, P. and Ganji, D.D., "Numerical analysis of mhd nanofluid flow and heat transfer in a circular porous medium containing a cassini oval under the influence of the lorentz and buoyancy forces", *Heat Transfer*, Vol. 51, No. 7, (2022), 6122-6138. https://doi.org/10.1002/htj.22582

30. Jalili, B., Jalili, P., Sadighi, S. and Ganji, D.D., "Effect of magnetic and boundary parameters on flow characteristics analysis of micropolar ferrofluid through the shrinking sheet with effective thermal conductivity", *Chinese Journal of Physics*, Vol. 71, (2021), 136-150. https://doi.org/10.1016/j.cjph.2020.02.034

31. Jalili, P., Narimisa, H., Jalili, B., Shateri, A. and Ganji, D., "A novel analytical approach to micro-polar nanofluid thermal analysis in the presence of thermophoresis, brownian motion and hall currents", *Soft Computing*, Vol. 27, No. 2, (2023), 677-689. https://doi.org/10.1007/s00500-022-07643-2

32. Jalili, B., Roshani, H., Jalili, P., Jalili, M., Pasha, P. and Ganji, D.D., "The magnetohydrodynamic flow of viscous fluid and heat transfer examination between permeable disks by agm and fem", *Case Studies in Thermal Engineering*, Vol. 45, (2023), 102961. https://doi.org/10.1016/j.csite.2023.102961

33. Jalili, P., Sharif Mousavi, S., Jalili, B., Pasha, P. and Ganji, D.D., "Thermal evaluation of mhd jeffrey fluid flow in the presence of a heat source and chemical reaction", *International Journal of Modern Physics B*, (2023), 2450113. https://doi.org/10.1142/S0217979224501133

34. Nagiredla, S., Joladarashi, S. and Kumar, H., "Rheological properties of the in-house prepared magneto-rheological fluid in the pre-yield region", *International Journal of Engineering, Transactions B: Applications*, Vol. 35, No. 11, (2022), 2238-2246. doi: 10.5829/IJE.2022.35.11B.19.

35. Pasha, P., Nabi, H., Peiravi, M., Pourfallah, M. and Domiri Ganji, D., "The application of analytical methods in the investigation effects of magnetic parameter and brownian motion on the fluid flow between two equal plates", *International Journal of Engineering, Transactions A: Basics*, Vol. 34, No. 10, (2021), 2341-2350. doi: 10.5829/IJE.2021.34.10A.15.

36. Tajik Jamal-Abad, M., "Analytical investigation of forced convection in thermally developed region of a channel partially filled with an asymmetric porous material-ltne model", *International Journal of Engineering, Transactions A: Basics*, Vol. 29, No. 7, (2016), 975-984.
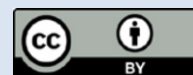
Persian Abstract

چکیده

در این مقاله، معادلات حاکم بر جریان فرومغناطیسی ثابت بررسی شده است. نیروی لورنتس، این جریان فروسیال را در یک دریچه نیمه متخلخل مهار می کند. آنالیزها بر روی سه سیال زیر ذره‌ای انجام شد: نفت سفید و خون، آب و مگنتیت. مدلسازی در سیستم مختصات دکارتی با استفاده از معادلات مربوطه بررسی شده است. در قسمت پایینی این کانال باید کمی نازک شدن در نظر گرفته شود. در این تحقیق از دو روش اکبری- گنجی و روش اجزاء محدود برای حل معادلات استفاده شده است. معادلات دیفرانسیل غیرخطی با استفاده از دو روش فوق حل می شوند. در مدل اجزاء محدود، اثر تغییر عدد هارتمن و عدد رینولدز بر سرعت جریان و مشتقات سرعت و تنش برشی سیال بررسی شده است. با افزایش عدد هارتمن، سرعت در هر دو جهت کاهش می یابد. عدد رینولدز در پارامترهای لغزش مختلف تغییر می کند که رفتار مخالف را برای دو جهت نشان می دهد. همچنین اثر ناچیز کسر حجمی نانوذرات بر سرعت و مشتقات آن و تنش برشی بررسی شده است. نتایج حل معادلات با دو روش فوق با روش هموتوپی مقایسه شده است. نتایج به دست آمده با استفاده از روش اکبری-گنجی و روش اجزاء محدود و مقایسه آنها با تحقیقات قبلی منجر به مطابقت کامل شده است که نشان دهنده کارایی تکنیک های مورد استفاده در این تحقیق است.